Records of Natural Products

www.acgpubs.org
ORIGINAL ARTICLE

GNPS molecular networking-guided discovery of antifungal butenolides from the endophytic fungus *Aspergillus* sp. FH-1 of *Valeriana officinalis* L.

Hao Fan[1], Xin Wang[1], Yinhan Teng[1], Pingping Wu[2], Haifang Wang[3], Yuze Li[1], Henglei Niu[1], Wei Wang[1], Xiaome Song[1], Qing Chang[4*] and Dongdong Zhang[1*]

[1]School of Pharmacy, Shaanxi University of Chinese Medicine, Shaanxi Key Laboratory of Research and Application of "Taibai Qi Yao", Xianyang, 712046, China
[2]Department of Pharmacy, Jinjiang Municipal Hospital (Shanghai Sixth People's Hospital Fujian Campus), Quanzhou, 362200, China
[3]Shaanxi University of Chinese Medicine, Shaanxi Key Laboratory of Integrated Traditional and Western Medicine for Prevention and Treatment of Cardiovascular Diseases, Institute of Integrative Medicine, Xianyang, 712046, China
[4]Affiliated Hospital of Shaanxi University of Chinese Medicine, Xianyang, 712000, China

Abstract: Guided by an integrated GNPS molecular networking strategy, the chemical investigation of endophytic fungus *Aspergillus* sp. FH-1 (isolated from *Valeriana officinalis* L.) led to the discovery of four butenolides (**1**–**4**). Their structures were elucidated through comprehensive spectroscopic data analysis, including HRESIMS, 1D/2D NMR and ECD, revealing two new congeners, asperianas A (**1**) and B (**2**), along with the known analogues **3** and **4**. Notably, compounds **1** and **3** exhibited significant antifungal activity against *Colletotrichum gloeosporioides*, with EC_{50} values of 19.23 ± 1.14 and 43.36 ± 1.12 μg/mL, respectively.

Keywords: *Aspergillus* sp. FH-1, GNPS molecular networking, butenolides, antifungal

Cite this article as:
Fan et al. GNPS molecular networking-guided discovery of antifungal butenolides from the endophytic fungus *Aspergillus* sp. FH-1 of *Valeriana officinalis* L.. (2026). *Records of Natural Products*, 20(3):e25123778

Received: *31 December 2025*
Revised: *10 February 2026*
Accepted: *10 February 2026*
Published: *03 March 2026*

1 Introduction

Fungal diseases cast a long shadow over global agriculture, inflicting severe damage on cash crops and incurring substantial economic losses each year (Fisher et al., 2018; Wang et al., 2022; Khan & Korban, 2022). To counter this persistent threat, the search for effective antifungal agents is of paramount importance. Among natural product leads, butenolide derivatives have attracted significant interest from researchers in both plant pathology and chemistry, thanks to their demonstrated antifungal properties. The unique architecture of these compounds—notably their phenyl and benzyl disubstitution pattern—is strongly linked to their bioactivity, positioning them as a valuable lead structure for next-generation agrochemical development (Vanti et al., 2021; Fan et al., 2026b, 2024a).

Based on the observed antifungal activities of butenolide derivatives (Fan et al., 2024a, 2024b, 2020), the endophytic fungus *Aspergillus* sp. FH-1 was investigated for its secondary metabolites. A GNPS-based molecular networking strategy (Phelan, 2020) led to the targeted isolation of four butenolides. Among them, two new compounds, designated asperiana A (**1**) and B (**2**), were characterized alongside known analogues **3** and **4** (Figure 1). In antifungal assays against *Colletotrichum gloeosporioides*, compounds **1** and **3** demonstrated potent activity, exhibiting inhibition 2.6-fold and 1.1-fold stronger, respectively, than the positive control carbendazim.

2 Materials and Methods

General experimental procedures; Fungal Strain, Cultivation, Extraction and Isolation, and GNPS molecular networking were listed in the Supplementary Information.

2.1 Plant Material and Fungal Strain

The endophytic fungal strain FH-1, used in this study, was isolated from surface-sterilized fresh rhizomes of *Valeriana officinalis* L. The host plant material was collected in the

*Corresponding Authors: Qing Chang.
Email: cqbreeze@126.com; Dongdong Zhang.
Email: zhangnatprod@163.com

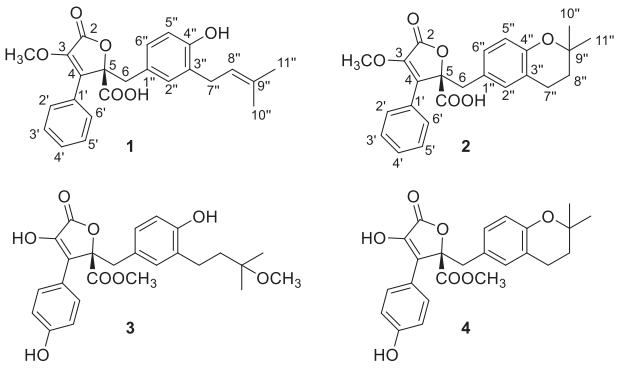

Figure 1. Chemical structure of compounds **1–4** from *Aspergillus* sp. FH-1

Taibai Mountain area within the Qinling range, Shaanxi Province, China. Botanical identification of *V. officinalis* was confirmed by Prof. Wei Wang at the School of Pharmacy, Shaanxi University of Chinese Medicine, and a voucher specimen (No. XC20241001) was deposited accordingly. For fungal identification, genomic DNA was extracted from the pure culture of strain FH-1, and the internal transcribed spacer (ITS) region of the ribosomal RNA gene was amplified by polymerase chain reaction (PCR). The resulting ITS sequence was submitted to the GenBank database under accession number KF367546.1. Sequence comparison using the NCBI BLAST algorithm and subsequent phylogenetic analysis supported the classification of the isolate as a species of *Aspergillus*. A reference culture of strain FH-1 has been preserved at the Key Laboratory of Taibai Qiyao Research and Application, School of Pharmacy, Shaanxi University of Chinese Medicine.

2.2 Antifungal Activity Assay

Antifungal activities of the purified compounds were evaluated against *Colletotrichum gloeosporioides* based on a mycelial growth inhibition assay. A concentration series of each compound (100, 50, 25, 12.5, and 6.25 μg/mL) was prepared in triplicate and incorporated into Potato Dextrose Agar (PDA) medium. Sterile water and carbendazim were used as the negative and positive controls, respectively. Mycelial disks (5 mm diameter), excised from the actively growing edge of a fungal colony, were aseptically inoculated onto the center of each PDA plate. Following incubation at 28°C for 3 days, colony diameters were measured using the cross-intersection method, and the mycelial growth inhibition rate was calculated accordingly.

2.3 Spectroscopic Data of Asperianas A (**1**) and B (**2**)

Asperiana A (**1**): White amorphous powder, HRESIMS: *m/z* 407.1493 $[M\text{-}H]^-$, (Calculated for 407.1495 $[M\text{-}H]^-$). ^{1}H NMR (Methanol-d_4, 400 MHz) and ^{13}C NMR (Pyridine-d_5, 100 MHz), see Table 1.

Asperiana B (**2**): White amorphous powder, HRESIMS: *m/z* 407.1494 $[M\text{-}H]^-$, (Calculated for 407.1495 $[M\text{-}H]^-$). ^{1}H NMR

Table 1. ^{1}H NMR and ^{13}C NMR nuclear magnetic resonance data of compounds **1** and **2** (δ in ppm, J in Hz, solvent: CD_3OD)

No.	1		2	
	δ_H, mult, (J in Hz)	δ_C, type	δ_H, mult, (J in Hz)	δ_C, type
2		170.0, C		170.0, C
3		141.9, C		142.0, C
4		128.3, C		125.6, C
5		87.0, C		87.1, C
6	3.46, s	39.6, CH_2	3.45, d (5.2)	39.6, CH_2
7		171.5, C		171.5, C
8	3.76, s	54.1, CH_3	3.78, s	54.1, CH_3
1′		128.6, C		128.4, C
2′ (6′)	7.72, d (7.2)	128.7, CH	7.69, d (7.2)	128.8, CH
3′ (5′)	7.46, m	129.9, CH	7.47, m	130.0, CH
4′	7.38, m	130.9, CH	7.39, m	130.4, CH
1″		131.8, C		132.0, C
2″	6.44, s	132.6, CH	6.45, m	132.8, CH
3″		125.1, C		121.6, C
4″		155.2, C		154.5, C
5″	6.53, s	115.2, CH	6.43, d (8.3)	117.6, CH
6″	6.53, s	129.9, CH	6.50, dd (8.3, 2.0)	129.9, CH
7″	3.10, m	28.9, CH_2	2.54, dd (11.7, 6.6)	23.3, CH_2
8″	5.08, t (7.2)	123.7, CH	1.70, t (6.7)	33.8, CH_2
9″		133.0, C		75.3, C
10″	1.65, s	26.2, CH_3	1.22, s	27.2, CH_3
11″	1.57, s	18.0, CH_3	1.22, s	27.2, CH_3

http://doi.org/10.25135/rnp.2512.3778
Rec. Nat. Prod. 2026, 20(3):e25123778

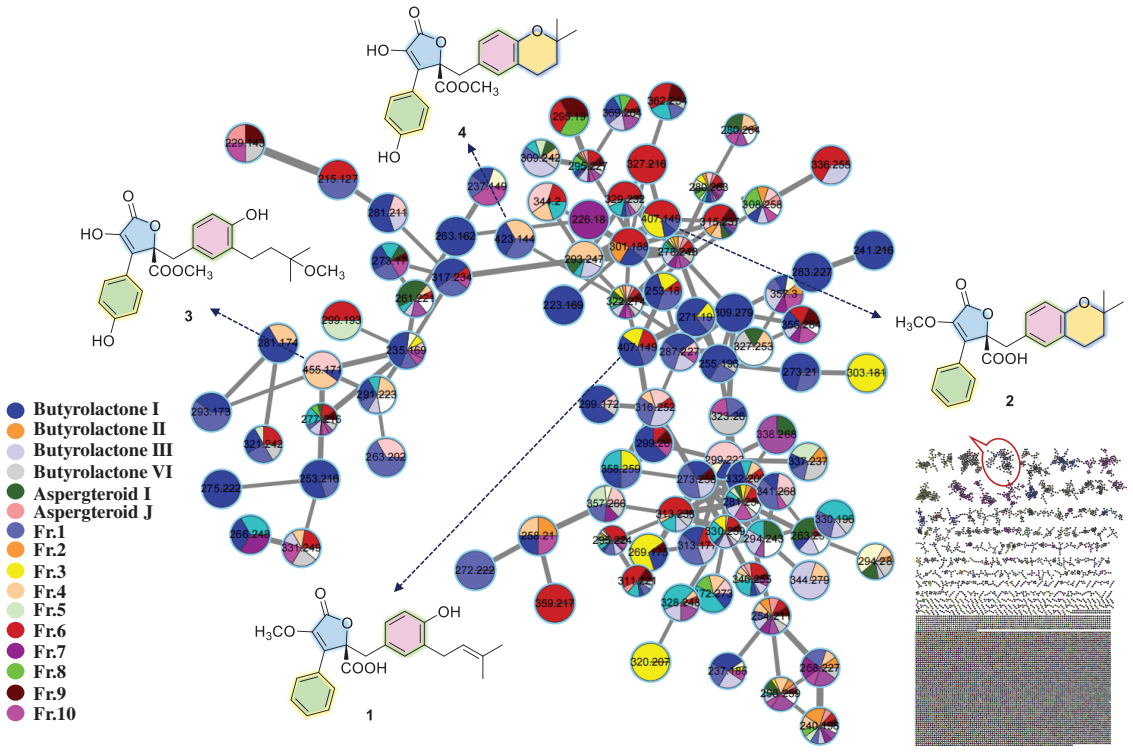

Figure 2. GNPS molecular network guiding the targeted isolation of butenolides

(Methanol-d_4, 400 MHz) and ^{13}C NMR (Pyridine-d_5, 100 MHz), see Table 1.

3 Results and Discussion

3.1 Targeted Identification of Butenolides Using GNPS Molecular Networking

To guide the targeted isolation of butenolides, a GNPS-based molecular network was constructed using a set of known butenolides—Butyrolactone I, Butyrolactone II, Butyrolactone III, Butyrolactone VI, Aspergteroid I, and Aspergteroid J—as reference compounds. By cross-referencing the MS/MS spectra of the primary fractions (Fr.1–10) against this reference set, a distinct butenolide-enriched cluster (Cluster 3) was identified. This cluster specifically comprised fractions Fr.3 and Fr.4, which were consequently prioritized for the focused screening and isolation of both novel and known butenolide derivatives (Figure 2).

3.2 Structure Elucidation

Compound **1** was isolated as white amorphous powder with a molecular formula of $C_{24}H_{24}O_6$, determined by its HR-ESI-MS *m/z* 407.1493 $[M-H]^-$ (calcd: 407.1495), indicating 13 degrees of unsaturation. The ^{1}H NMR spectrum indicated the signals of monosubstituted benzene ring at δ_H 7.72 (2H, d, J = 7.44 Hz, H-2′/6′), 7.46 (2H, m, H-3′/5′), an additional 1,3,4-trisubstituted benzene ring at δ_H 6.44 (1H, s, H-2″), 6.53 (1H, s, H-5″), 6.53 (1H, s, H-6″), and an olefinic proton at δ_H 5.08 (1H, t, J = 7.4 Hz, H-8″). The ^{13}C NMR spectrum exhibited 24 carbon resonances, classified as three methyls, two

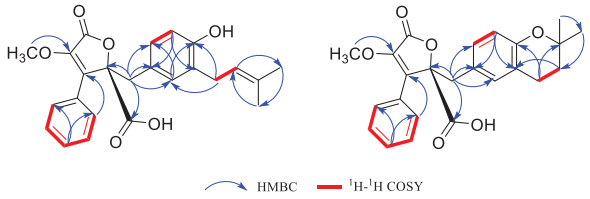

Figure 3. Structures and key 2D NMR correlations of compounds **1** and **2**

methylenes, nine methines, and ten nonprotonated carbons. A lactone [δ_C 170.0 (C)], a carboxy group [δ_C 171.5 (C)], two double bonds [(δ_C 141.9 (C), 128.3 (C) and 123.7 (CH), 133.0 (C)], an oxygenated carbon [δ_C 54.1 (-OCH_3)] and twelve aromatic signals were easily discerned (Table 1, Figure 3).

The planer structure of **1** was mainly determined by 2D NMR. Comprehensive analyses of the ^{1}H-^{1}H COSY spectrum revealed three spin-coupling systems: H-2′/H-3′/H-4′/H-5′/H-6′, H-5″/H-6″, H-7″/H-8″. The HMBC correlations from H-6 to C-5, C-7, C-1″, C-2″ and C-6″; H-5″ to C-1″ and C-3″; H-2″ to C-4″ and C-6″; H-7″ to C-2″ and C-4″; H-8″ to C-11″; H-11″ to C-10″; H-10″ to C-8″; H-8 to C-3. This completed the planar structures of compound **1**. Therefor compound **1** was deduced and named as asperiana A (Figure 1).

Compound **2** was isolated as white amorphous powder with a molecular formula of $C_{24}H_{24}O_6$, determined by its HR-ESI-MS *m/z* 407.1494 $[M-H]^-$ (calcd: 407.1495), indicating 13 degrees of unsaturation. The NMR data of compound **2** was extremely similar to **1**, indicating the same skeleton.

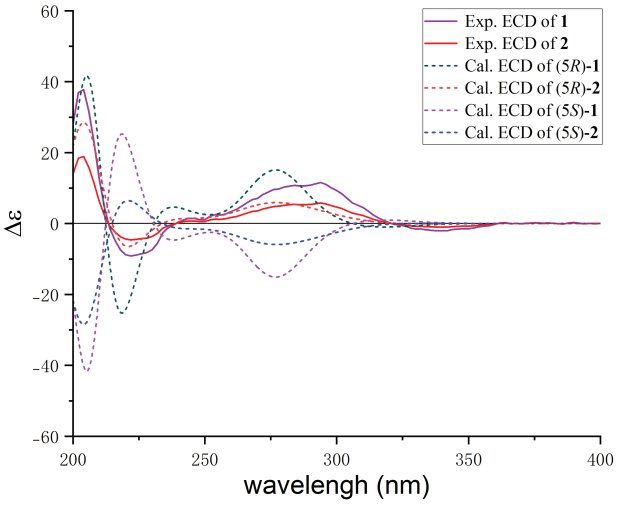

Figure 4. Experimental and calculated ECD spectra of compounds **1** and **2**

Compared with **1**, **2** showed additional signals of one methylene [δ_H 1.70 (2H, t, J = 6.7 Hz, H-8″); δ_C 33.8 (CH_2)] and one oxygenated quaternary [δ_C 75.3 (C)], while two olefinic carbons [δ_H 5.08 (1H, t, J = 7.4 Hz, H-8″); δ_C 123.7 (CH), 133.0 (C)] in **1** were absent in **2**. The ^{1}H-^{1}H COSY correlation of H-7″ and H-8″, combined with HMBC correlations from H-7″ to C-4″ and C-9″, H-8″ to C-3″, H-10″ to C-9″ and C-11″, H-11″ to C-8″ suggested a dihydropyran ring connected at C-3″-C-4″. Thus, the structure of **2** was established. Therefore compound **2** was deduced and named as asperiana B (Figure 1).

The absolute configurations of the new butenolides **1** and **2** were unambiguously assigned through comparison of their experimental electronic circular dichroism (ECD) spectra with the corresponding time-dependent density functional theory (TD-DFT) calculated spectra (Figure 4). For asperiana A (**1**), the experimental spectrum displayed a negative Cotton effect at 225 nM and a positive Cotton effect at 278 nm, which aligned excellently with the calculated spectrum for the 5*R* enantiomer (negative band at 220 nM, positive band at 270 nM). Similarly, the experimental ECD spectrum of asperiana B (**2**) exhibited a negative Cotton effect at 225 nM and a broad positive effect centered around 275 nM, convincingly matching the calculated profile for the 5*R* configuration (negative band at 222 nM, positive band at 272 nM). The consistent sign pattern of the Cotton effects observed for both compounds strongly supports their shared 5*R* configuration at the key stereogenic center (C-5), an assignment further corroborated by the proposed biosynthetic pathway for this class of butenolides (Fan et al., 2024a). Collectively, this detailed ECD analysis provides robust chiroptical evidence for the absolute stereochemistry of the new metabolites.

The structures of the **4** isolated butenolides were elucidated by comprehensive analysis of their spectroscopic data, including NMR and HRESIMS. Their identities were further confirmed by comparing their physicochemical properties and spectral data with those reported in the literature. Ultimately, the compounds were identified as aspernolide C (**3**) (Liu et al., 2018), aspernolide A (**4**) (Guo et al., 2016).

Table 2. The EC_{50} values (μg/mL) of compounds **1**–**4** against the mycelial growth of *C. gloeosporioides*

Compounds	EC_{50}	Compounds	EC_{50}
1	19.23 ± 1.14	**4**	>50
2	>50	Carbendazim*	49.58 ± 0.10
3	43.36 ± 1.12		

Note: *Positive control.

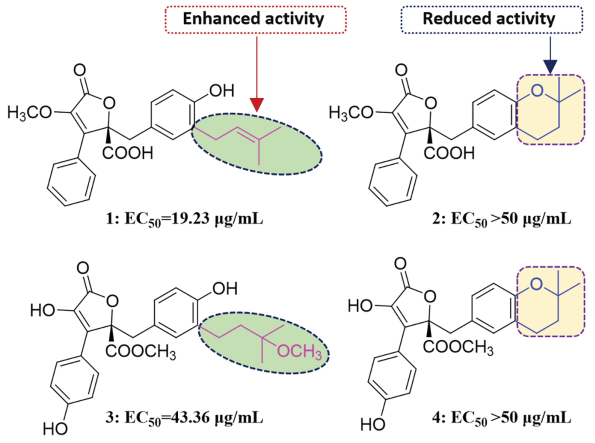

Figure 5. SAR analysis of butenolide compounds

3.3 Antifungal Activities of Compounds **1**–**4**

Antifungal activities are usually reported in natural or synthetic compounds (Fan et al., 2026b; Hu et al., 2018; Liu et al., 2024; Wang et al., 2022a, 2022b; Yang et al., 2025; Zheng et al., 2023; Zhong et al., 2016), in this study compounds **1**–**4** against the phytopathogen *Colletotrichum gloeosporioides* were preliminarily evaluated using the mycelial growth inhibition assay (Fan et al., 2024a). All compounds were tested at a series of five concentrations: 100, 50, 25, 12.5, and 6.25 μg/mL. The results, summarized in Table 2, indicated that compounds **1**–**4**. Notably, compounds **1** and **3** displayed stronger activity than the positive control, carbendazim.

3.4 Discussion of Structure-Activity Relationship

Antifungal assessment of the isolated butenolides revealed a clear structure–activity relationship (SAR) (Figure 5). Compounds **1** and **3**, which displayed stronger activity than the positive control carbendazim, both possess a flexible prenyl (or oxidized prenyl) side chain at the C-3″ position. This structural motif appears crucial for the observed potency. In contrast, the significantly reduced activity of compounds **2** and **4** coincides with the cyclization of this prenyl group with the adjacent phenolic hydroxyl at C-4″, forming a dihydropyran ring. This conformational constraint likely reduces molecular flexibility and may hinder key interactions, thereby diminishing antifungal efficacy.

http://doi.org/10.25135/rnp.2512.3778
Rec. Nat. Prod. 2026, 20(3):e25123778

4 Conclusion

In this study, the GNPS molecular networking strategy was successfully employed for the targeted isolation of antifungal butenolide metabolites from the endophytic fungus *Aspergillus* sp. FH-1, leading to the acquisition of four 4,5-disubstituted butenolide derivatives (Fan et al., 2022). These compounds displayed characteristic UV absorptions at approximately 220 and 306 nM and molecular weights around 400 Da, establishing useful criteria for the rapid screening of analogous structures. Antifungal activity analysis further revealed that the flexibility and spatial configuration of specific structural units, particularly the C-3″ side chain, played a critical role in activity modulation, thereby providing a clear foundation for the targeted structural optimization of butenolide-based antifungal agents.

Acknowledgement

The authors gratefully acknowledge Prof. Cuixian Zhang from Guangzhou University of Chinese Medicine for her valuable support in providing fungal culture conditions and GNPS-based molecular networking technical assistance.

Funding Statement

This work was supported by Shaanxi Provincial Department of Education Scientific Research Program Project (Grant No. 25JK0430); the Key Discipline Project of the National Administration of Traditional Chinese Medicine (Grant No. zyyzdxk-2023202); the Qinchuangyuan Traditional Chinese Medicine Industry Innovation Hub Project (Grant No. L2024-QCYZYYJJQ-X81, L2024-QCY-ZYYJJQ-X69); the Innovation Team Project of Shaanxi University of Chinese Medicine (Grant No. 2023-CXTD-05); Youth Innovation Team of Shaanxi Provincial Department of Education (Discovery and Application of Efficacy Substances in Taibai Qi Medicines); and the College Students' Innovation Training Program (Grant No. S202510716010).

Author Contributions

Hao Fan: Writing–original draft, Investigation, Data curation, Project administration. Xin Wang: Data curation. Yinhan Teng: Data curation. Pingping Wu: Data curation. Haifang Wang: Data curation. Yuze Li: Data curation. Henglei Niu: Data curation. Wei Wang: Data curation, Supervision. Xiaomei Song: Data curation, Supervision. Qing Chang: Writing–review & editing, Data curation, Supervision. Dongdong Zhang: Writing–review & editing, Data curation, Supervision.

Availability of Data and Materials

The authors declare that the data supporting the findings of this study are available within the paper and its Supplementary Information files. Should any raw data files be needed in another format they are available from the corresponding author upon reasonable request. Source data are provided with this paper.

Conflicts of Interest

The authors declare that they do not have any conflict of interest.

Supporting Information

Supporting Information accompanies this paper on http://www.acgpubs.org/journal/records-of-natural-products.

ORCID

Hao Fan: 0000-0002-0822-1639
Xin Wang: 0009-0001-3502-3822
Yinhan Teng: 0009-0007-6535-7288
Pingping Wu: 0009-0001-2491-6852
Haifang Wang: 0000-0002-3320-4398
Yuze Li: 0000-0001-7571-3214
Henglei Niu: 0009-0001-8900-8759
Wei Wang: 0000-0002-4699-0498
Xiaomei Song: 0000-0003-1906-1578
Qing Chang: 0009-0002-0709-1577
Dongdong Zhang: 0000-0003-0956-1261

References

Fan, Z., Hu, Z. Z., Chen, Y. F., Huang, D. Y., Shi, Y. & Qian, Y. M. (2026a). A new antifungal α-pyrone secondary metabolite isolated from the tobacco-derived fungus *Aspergillus* aculeatus Aa-1. *Records of Natural Products*, *20*, e25113719. DOI: 10.25135/rnp.2511.3719.

Fan, H., Li, Y. Z., Liang, X. F., Yan, S. T., Cui, Y. W., Zhang, H. W., Huang, W. L., Yang, X. J. & Song, X. M. (2020). Chemical constituents isolated from *Valeriana officinalis* L. *Biochemical Systematics and Ecology*, *93*, 104143. DOI: 10.1016/j.bse.2020.104143.

Fan, H., Shao, X. H., Wu, P. P., Hao, A. L., Luo, Z. W., Zhang, M. D., Xie, J., Peng, B. & Zhang, C. X. (2024a). Exploring brominated aromatic butenolides from *Aspergillus terreus* EGF7-0-1 with their antifungal activities. *Journal of Agricultural and Food Chemistry*, *72*, 19869–19882. DOI: 10.1021/acs.jafc.4c04728.

Fan, H., Shao, X. H., Zhang, Z. K., Ni, C., Feng, C., Wei, X., Zhu, J. Q., Li, X. H. & Zhang, C. X. (2024b). Penicilloneines A and B, quinolone-citrinin Hybrids from a starfish-derived *Penicillium* sp. *Journal of Natural Products*, *87*, 705–712. DOI: 10.1021/acs.jnatprod.3c00765.

Fan, H., Wei, X., Si-Tu, M. X., Lei, Y. H., Zhou, F. G. & Zhang, C. X. (2022). γ-Aromatic butenolides of microbial source—a review of their structures, biological activities and biosynthesis. *Chemistry & Biodiversity*, *19*, e202200208. DOI: 10.1002/cbdv.202200208.

Fan, H., Wu, P. P., Wang, X., Li, Y., Deng, C., Wang, W., Song, X. M., Zhang, X. & Zhang, D. (2026b). OSMAC-activated and GNPS-guided investigation of alkaloids from an endophytic fungus *Aspergillus* sp. FH-1 of *Valeriana officinalis* L. *Biochemical Systematics and Ecology*, *124*, 105151–105158. DOI: 10.1016/j.bse.2025.105151.

Fisher, M. C., Hawkins, N. J., Sanglard, D. & Gurr, S. J. (2018). Worldwide emergence of resistance to antifungal drugs challenges human health and food security. *Science*, *360*, 739–742. DOI: 10.1126/science.aap7999.

Guo, F., Li, Z., Xu, X., Wang, K., Shao, M., Zhao, F., Wang, H., Hua, H., Pei, Y. & Bai, J. (2016). Butenolide derivatives from the plant endophytic fungus *Aspergillus terreus*. *Fitoterapia*, *113*, 44–50. DOI: 10.1016/j.fitote.2016.06.014.

Hu, L., Wang, H., Xia, T. T., Fang, B., Shen, Y., Zhang, Q., Tian, X. H., Zhou, H. P., Wu, J. Y., Tian, Y. Y. (2018). Two-photon-active organotin (IV) complexes for antibacterial function and superresolution bacteria imaging. *Inorganic Chemistry*, *57*, 6340–6348. DOI: 10.1021/acs.inorgchem.8b00413.

Khan, A., Korban, S. S. (2022). Breeding and genetics of disease resistance in temperate fruit trees: Challenges and new opportunities. *Theoretical and Applied Genetics*, *135*, 3961–3985. DOI: 10.1007/s00122-022-04093-0.

Liu, M. T., Sun, W. G., Wang, J. P., He, Y., Zhang, J., Li, F. & Zhang, Y. (2018). Bioactive secondary metabolites from the marine-associated fungus *Aspergillus terreus*. *Bioorganic Chemistry*, *80*, 525–530. DOI: 10.1016/j.bioorg.2018.06.029.

Liu, J. J., Xiong, M. M., Zhai, X. Y., Zhang, J. X., Li, Z. & Lv, J. H. (2024). A new diphenyl ether derivative from an endolichenic fungus *Preussia Africana*. *Records of Natural Products*, *18*, 245–250. DOI: 10.25135/rnp.446-2401.3027.

Phelan, V. V. (2020). Feature-based molecular networking for metabolite annotation. *Methods in Molecular Biology*, *2104*, 227–243. DOI: 10.1007/978-1-0716-0239-3_13.

Vanti, G. L., Leshem, Y. & Masaphy, S. (2021). Resistance response enhancement and reduction of *Botrytis cinerea* infection in strawberry fruit by *Morchella conica* mycelial extract. *Postharvest Biology and Technology*, *175*, 111470. DOI: 10.1016/j.postharvbio.2021.111470.

Wang, R. N., Li, R. Y., Li, F. K., Zheng, P., Wang, Z. & Qian, S. H. (2022a). Glycerol and antimicrobial peptide-modified natural latex for bacteriostasis of skin wounds. *ACS Omega*, *8*, 1505–1513. DOI: 10.1021/acsomega.2c07008.

Wang, Z., Sui, Y., Li, J., Tian, X. & Wang, Q. (2022b). Biological control of postharvest fungal decays in citrus: A review. *Critical Reviews in Food Science and Nutrition*, *62*, 861–870. DOI: 10.1080/10408398.2020.1829542.

Yang, X. Z., Huang, Z. X., Ding, K. K., Yang, H. L., Wang, L. R., Xia, Q., Hu, R., Shi, G., Xu, B. J., Qin, A. J. (2025). Near-infrared organic photosensitizers with aggregation-induced emission and switchable fluorescence for fungal infection therapy. *Science China Chemistry*, *68*, 1426–1433. DOI: 10.1007/s11426-024-2325-2.

Zheng, P., Li, R. Y., Li, F. F. K., Wang, R. N. & Qian, S. H. (2023). Exploration of biological properties and antibacterial action against escherichia coli and staphylococcus aureus of (LLKK)3-derived peptides. *ChemistrySelect*, *12*, e202300355. DOI: 10.1002/slct.202300355.

Zhong, Y. M., Ni, Y. H., Li, S. F. & Wang, M. F. (2016). Chain-like Fe_3O_4@resorcinol-formaldehyde resins-Ag composite microstructures: Facile construction and applications in antibacterial and catalytic fields. *RSC Advances*, *9*, 15831–15837. DOI: 10.1039/c5ra27605e.